

DEPICTION OF DETRIMENTAL METALLURGICAL EFFECTS IN GRADE 304 AUSTENITIC STAINLESS STEEL ARC WELDS

RATI SALUJA¹ & K. M. MOEED²

¹Associate Professor, Department of Mechanical Engineering, Goel Institute of Technology
and Management, Lucknow, India

²Principal, University Polytechnic, Integral University, Lucknow, India

ABSTRACT

Efforts have been made to integrate fundamental microscopic behaviour and metallurgical transformations of Grade 304 Austenitic stainless steel during solidification. Incomplete mixing during solidification of Grade 304 steel in weld pool initiates segregation that encourages the dendritic envelope motion regulated by the enlargement of dendrite tips. High segregation of chromium and molybdenum, lead to the formation of secondary ferrite that increases tendency of accumulation of intermetallic phases. Micro and macro cracks with different orientations also occur in various sections of the weld, because of low melting liquid phases in the primary weld zone or enveloping HAZ. It aggravates grain boundaries to split under the thermal and shrinkage strain during metallurgical changes. Solid-state transformation of ferrite to austenite results in separation of solidification boundaries from grain boundaries thus reduces possibility of hot cracking. But probability of fissuring in the weld HAZ in fully austenite welds is higher than in ferrite containing welds. Contending variables adjoin complexity, hence the primary intention of this review is to correlate microstructural developments of Grade 304 steel under the influence of metallurgical variations.

KEYWORDS: Austenitic Stainless Steel, Delta Ferrite, Embrittlement, Hot Cracking, Segregation & Solidification Cracking

Received: Aug 20, 2018; **Accepted:** Sep 10, 2018; **Published:** Sep 29, 2018; **Paper Id.:** IJMPERDDEC201825

1. INTRODUCTION

The knowledge of welding metallurgy is imperative as overall mechanical properties of parent metal are influenced by the metallurgical developments of the weld deposit and HAZ [1]. Solidification phases (A, AF, FA, F) are characterized as a key determinant of hot cracking susceptibility (HCS) for Austenitic stainless steels (ASSs). During equilibrium, the liquidus projection commences at the peritectic reaction ($\delta + L \leftrightarrow \gamma$) on Fe-Ni system and ends with the eutectic reaction ($L \leftrightarrow \gamma + \delta$) on the Fe-Cr-Ni ternary system for 17.2 weight percent chromium and 11.9 weight percent Nickel as shown in Figure 1 [2]. The prime purpose of Nickel in ASSs welds is to stabilize austenite phase, whether chromium is a ferrite promoting constituent. Weld having less than 12.7% chromium will form at least some austenite in gamma loop results in sigma phase embrittlement, whether weld having more than 16 wt% chromium will be fully ferritic at elevated temperatures [3]. The sigma phase precipitation also significantly affects the properties of Grade 304 Austenitic Stainless Steels (ASSs). It increases chromium insolubility and reduces the corrosion resistance. Hence it becomes mandatory to restrain the formation of chromium carbides by retaining a ferrite level in the prescribed range [4].

The continuous progression of the chromium equivalent to nickel equivalent ratio (duplex microstructure) ends in a transformation of the solidification mode from Austenite-Ferritic (AF) to Ferrite-Austenitic (FA) [5]. If the duplex structure (AF and FA) adjusts within 5–10% volume ferrite (F), results with hot cracking resistant finished weld [6]. Therefore, lower percentage of ferrite is particularized to minimize the probability of hot cracking during solidification, during post weld heat treatment or in service.

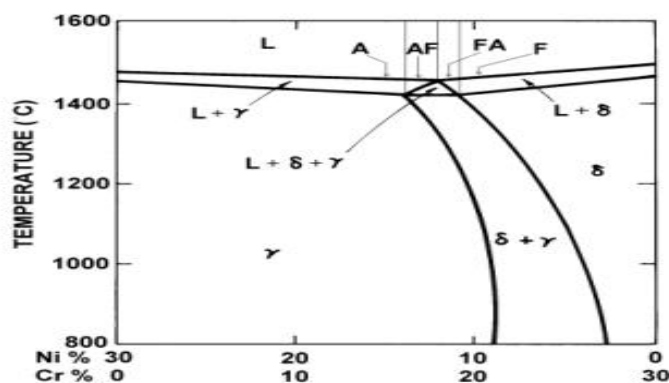


Figure 1: Vertical Section of the Fe–Cr–Ni Phase Diagram at 70% Fe [2]

The concern is also that duplex microstructure contains comparatively lesser volume portion of retained ferrite, designated as delta ferrite [7, 8]. The reduction in ferrite level is time subservient phenomenon, as the determination is diffusion controlled and the primary solidification segregation extent in both austenite and ferrite is also an agent in the degree of resolution of ferrite. Three categories of hot cracking during welding of Grade 304 steel are solidification cracking, liquification cracking and ductility dip cracking [9, 10]. While comparing to other detrimental effects caused by cracking, solidification cracking in the weld is reckoned utmost detrimental amongst all kinds of cracking [11]. The cracking above the location, temperature is known as super solidus or solidification cracking and in the solid state, termed as sub-solidus cracking [12]. Therefore, this review briefs general understanding for speculation of microstructure mechanisms of Grade 304 weld metal under arc welding and, the possible synergy between metallurgical developments and their outcomes.

2. METALLURGICAL EFFECTS OF WELDING

This Emphasis is placed to understand the root causes of various metallurgical defects with respect to their commencement, growth, outcome and prominence with a view to assess controlling factors for their regulation. Composition, solidification strain and solidification model are found the key determinants for regulation of weld-ambiguities [14].

2.1 Eminence of Solidification Cracking in Grade 304L Weld

Hot-Cracking Susceptibility (HCS) of ASSs is considered one of the most significant factors affecting weldability. Better resistance to hot cracking in arc welds can be experienced either from Ferritic-Austenitic (FA) or Ferritic (F) solidification mode [10]. As the solid-state transformation experiences $\delta \rightarrow \gamma$ interfaces ($A \rightarrow F$), better cracking resistance can be obtained with δ/γ (FA) interfaces than δ/δ (F) or γ/γ (A) interfaces [13]. Crack formation initiates as a film cannot endure the volumetric compression strain [15-18]. Hammar–Svensson diagram demonstrates the compositions according to hot cracking susceptibility [5]. Extremely susceptible weld compositions with a lower P+S limit of 0.01–0.015 wt.% are plotted on the X-axis holding $Cr_{eq}/Ni_{eq} < 1.5$, resulting in A-mode [19]. So, constituents with $Cr_{eq}/Ni_{eq} > 1.5$ conversely with

$P + S < 0.01$ wt% are 'not susceptible.' Although, the cracking proclivity speedily increases when the Cr_{eq}/Ni_{eq} ratio < 1.5 , retaining $P + S < 0.01$ wt% [19,20]. Lundin quantified the compositions by Total Crack-Length (TCL), as 'highly susceptible' if $TCL > 2.5$ mm, 'susceptible' if $1.5 < TCL < 2.5$ mm, and 'not susceptible' if $TCL < 1.5$ mm. The FA - solidification mode region, owning Cr_{eq}/Ni_{eq} within 1.5-1.6, was identified possessing a cracking vulnerability intermediate between that of the A- mode and FA/F-mode [21].

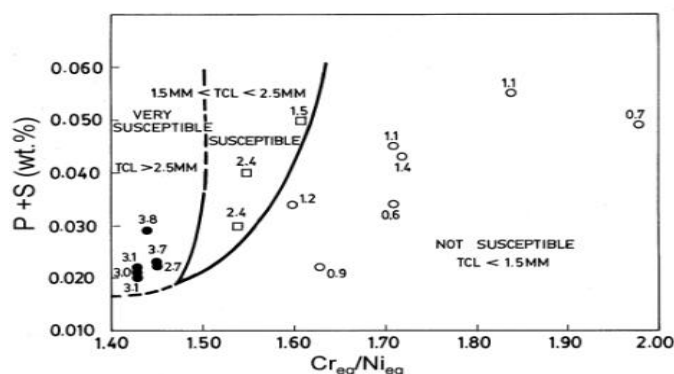


Figure 2: Hammar-Svensson Equation Demonstrating Solidification is Cracking Tendency in Austenitic Stainless Steel Welds [5]

2.1.1 Effects of P, S, Si, Nb, C and N on Hot Cracking Susceptibility of Fully Austenitic Alloys

Weld contains consistent alloys with variables melting points as displayed in Table 1. Solidifying dendrites rejects low point eutectics (Eutectic Fe-FeS, Eutectic Ni-NiS, Eutectic Fe-Fe₂Si, Eutectic NiSi-Ni₃Si₂, NiSi γ , Eutectic Fe-Fe₃P, and Eutectic Ni-Ni₃P) and produce a lean layer of molten metal away from weld pool. These constituents, boost HCS, originates when P+S segregate at the austenitic grain boundaries at the time of solidification [22-27]. The materials having Ferritic/Ferritic-Austenitic solidification mode beside a Chromium-Nickel equivalent ratio beyond 1.6 were considerably receptive to P+S with 0.04 wt.%, a contrast to A-mode materials [6].

Table 1: Partition Coefficients and Melting Points of Low Melting Phases of Hot Cracking Promoting Elements for Grade 304 L Steel [15,16]

Constituent	Temperature °C	Partition Coefficient		Low Melting Phases	
		δ	γ	Structure	Melting Points °C
S	1365	0.091	0.035	Eutectic Fe-FeS, Eutectic Ni-NiS	988 630
Si	1300	0.77	0.52	Eutectic Fe-Fe ₂ Si, Eutectic NiSi-Ni ₃ Si ₂ , NiSi γ	1212 964 996
P	1250	0.25	0.125	Eutectic Fe-Fe ₃ P, Eutectic Ni-Ni ₃ P	1048 875

Ogawa and Tsunetomi, had attempted experimental investigation to understand the influence of alloying constituents on ASSs for determination of HCS. Emphasis was placed to improve HCS with a view to the keep impurity level of $P + S < 0.002\%$, along with reducing silicon. They stated that HCS amplifies noticeably if $P > 0.015\%$. They explored that HCS enhances speedily if $S > 0.010\%$. HCS amplifies linearly until Si content reaches to 1.5%, then lowers sharply, if she exceeds 2.0% due to presence of surplus ferrite. N has diverging influence on HCS, in the presence of Nb. HCS reduces significantly with an increase in C in the presence of Nb. Thus, it can be concluded that HCS in Grade 304 ASSs can be enhanced by (1) decreasing $P + S$ to $< 0.002\%$, (2) reducing Si, (3) increasing C if Nb is high, and (4)

enhancing Nif Nb is absent [28].

2.2 Prominence of Heat Affected Zone Cracking in Grade 304L SS

Table 2 the heat affected zone in ASSs generally consist of homogeneous parent metal (except multi-pass and repair welds), that suffers with uneven thermal cycle. HAZ experiences lesser heat exposure and cooling in compare to fusion zone. Liquification cracking is witnessed in the partially melted zone of Grade 304 steels at elevated temperatures, whether the probability of ductility dip cracking is detected in the HAZ. Cracks originated are found intergranular and initiate in the pervasion of a liquid film along with the grain boundaries [29]. Occurrence of liquification and ductility dip cracking is found in HAZ of a single pass otherwise in the initial passes of a multi-pass joint. Various possible modes of HAZ sensitization are mentioned in Table 2.

Table 2: Four Potential Modes of HAZ Sensitization [32, 33]

Model	Imposed Thermal Cycle	Sensitized Structure	Relevant Weld Processing Conditions
1	Double thermal cycle, with heating above the A1, temperature during first annealing succeeded with a second heating step to temperatures about 650°C and 700°C.	Martensite with Chromium rich carbides on austenitic grain interfaces	Low temperature heat affected zone (LTHAZ) of weld deposited on base metal containing untempered martensite
2	Double thermal cycle with heating above the A1 temperature, followed by a second heating step to temperatures range 550°C – 650°C.	Martensite with Chromium rich carbides on austenitic grain interfaces.	Multiple weld positioned in such a way that HAZ of 2 nd pass overlaps the HAZ of standard Pass
3	Heating to temperature close to the liquidus, followed by rapid cooling.	Coarse grained delta ferrite with precipitation of chromium carbides at continuous ferrite-ferrite grain boundaries.	High temperature heat affected zone (HTHAZ) generated by single pass low heat input weld, arc strikes or areas with excessive fillet weld overlap.
4	Heating to a temperature close to the liquidus, followed by very slow cooling.	Carbide precipitation at austenitic grain interfaces throughout solidification.	High temperature heat affected zone (HTHAZ) generated by single pass welds performed at excessively high heat input levels

Two fundamental factors that participate in the initiation and development of a fluid film in the HAZ cracking are 1) Segregation of low-melting eutectics that lowers the solidus temperature and 2) The efficiency of fluid to penetrate from the fusion zone and wetting of grain boundaries [30, 31]. Figure 3 displays the association between P+S ratio along with chromium equivalent to nickel equivalent (Cr_{eq}/Ni_{eq}) to the HAZ cracking susceptibility of the weld at an applied strain level of 4.9% [31]. The solid line defines the boundary between primary austenitic and ferritic solidification. It shows that for ferrite levels greater than 3 FN, the cracking tendency is low. The cracks in all the specimens were found intergranular and oriented normal to the fusion line [9, 33].

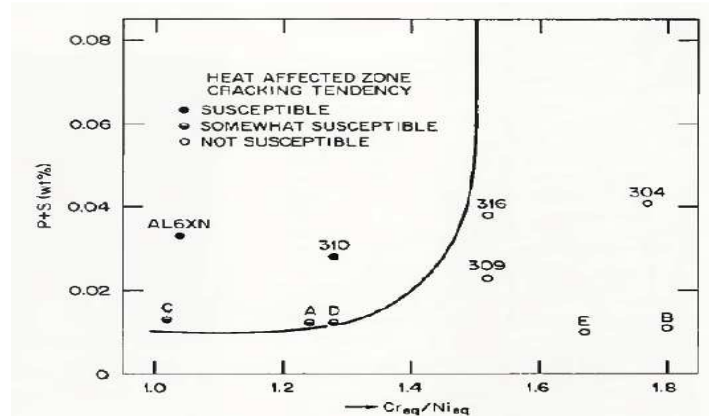


Figure 3: HAZ Cracking Tendency as a Function of (P+S) and Cr_{eq}/Ni_{eq} for ASSs [33].

2.3 Fissuring in Multipass, Ferrite-Containing Grade 304 Welds

Fissures may produce if the strain inflicted in the weld bead transcends the strain limit of the microstructural zone, also known as "Hazard HAZ" as displayed Figure 4. "Hazard HAZ" region in the fully austenitic welds is wider than in the ferrite containing welds. Therefore, the probability of fissuring in the weld HAZ in fully austenitic welds is higher than in ferrite containing welds [45].

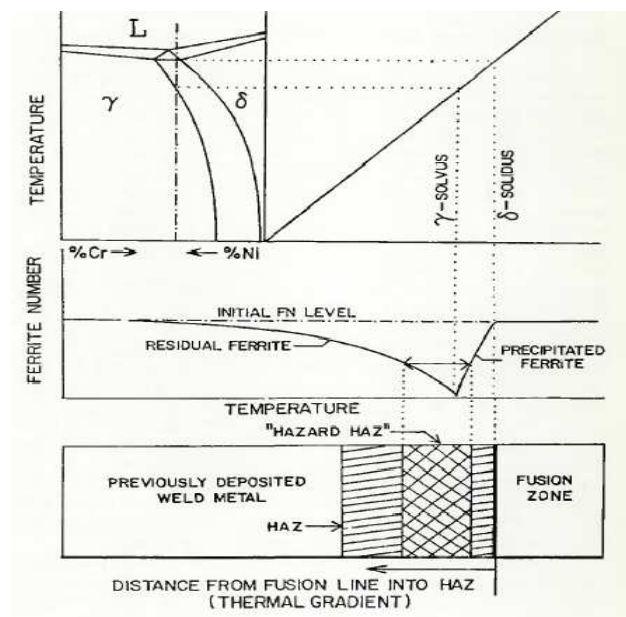


Figure 4: Schematic Location of "Hazard HAZ" Region and its Relationship to the Phase Diagram [45]

Ductility also decreases sharply and intergranular fissures occur when the strain intolerance is exceeded during the cooling fraction of the thermal cycle. The temperature range in which the ductility decreases to the utmost ranges from 1800°F (approximately) to the solidus temperature as displayed in Figure 5 [46]. For the low ferrite potential material, residual ferrite transforms into austenite through a solid state reaction if the material is reheated above γ -solvus [47]. Ferrite, having a higher solubility for low melting eutectics (S, P, and Si) absconds these impurities, as it transforms to austenite ($F \rightarrow A$). These "released harmful eutectics" further extend by diffusion and grain boundary migration to the austenite core and austenite grain boundaries, degrading their ductility and intensifying fissuring trend [43]. Increasing the

temperature above the 7-solvus, revived delta ferrite gets reabsorbed whether below the 7-solvus it reconverts to austenite. Since the 7-solvus temperature is lower for a high ferrite potential metal, the "Hazard HAZ" section is thinner, in contrast to the lower ferrite content metal. Thus, it can be summarized that the amplitude of the "Hazard HAZ" and the ferrite content therein depends upon the ferrite potential of the welding filler material and the thermal conditions coaxed [47]. If not, fissuring may befall in the HAZ if welding conditions dignify sufficient restraint. Microscopy is also useful to detect brittle phases in those austenitic stainless steels subject to high temperature cycles and containing high levels of δ -ferrite, due to possible spinodal decomposition ($\delta \rightarrow \alpha + \alpha'$) or σ -phase formation [48].

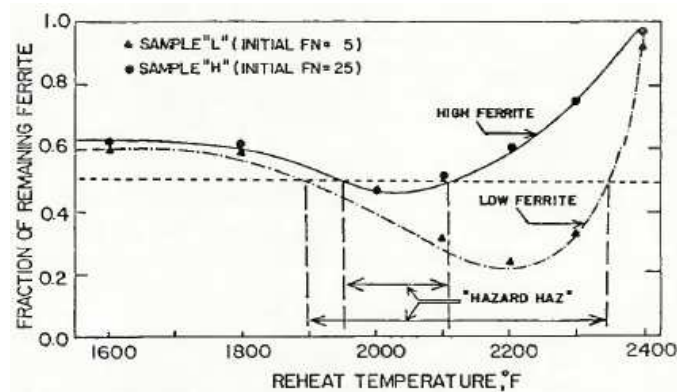


Figure 5: Effect of Preheat Temperature on the Fraction of Ferrite Remaining in Austenitic SS Weld-Bead [46]

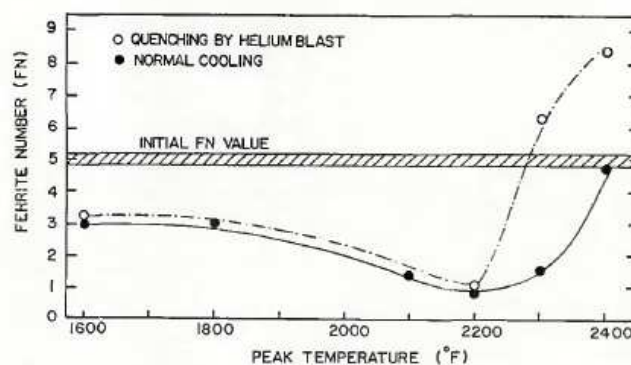


Figure 6 (a): Influence of Peak Temperature over the FN for Austenitic Stainless Steel Weld L (FN5)

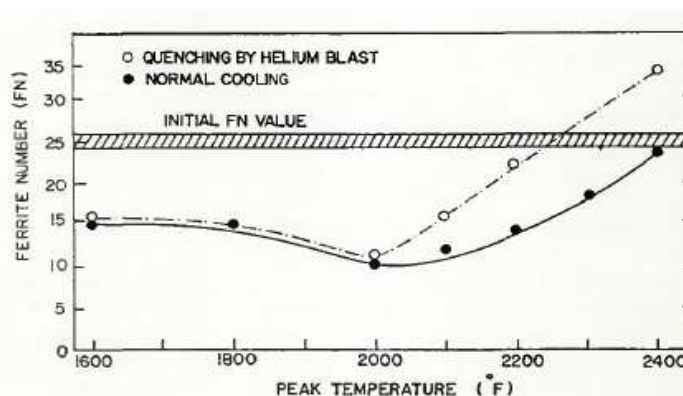


Figure 6 (b): Influence of Peak Temperature over the FN for Austenitic Stainless Steel Weld H (FN25) [53]

2. 4 Consequences of Delta Ferrite Permanence in 304 Welds

Welds having lower Ferrite Number (FN) are more sensitive to cracking than the welds having high ferrite numbers. Moreover, the ferrite number in the fissured area of the weld Heat Affected Zone (HAZ) was found lesser than the majority of the weld deposit area for 304L ASSs weld joints. Microscopic analysis of the fissured welds reveals the presence of the fissures in the zone adjacent to, though not conterminous with, the fusion area of the weld joint of 304 steel. It deciphers the cracking temperature range to be from 1065°C to 1315°C [21]. Figure 6 (a) and 6 (b) present plots for the low ferrite (FN5) and the high ferrite weld (FN25) as a function of peak temperature and cooling rate. The results of the determinations present that the ferrite number reduces with a growth of peak temperature from 1204°C and then increases again as the temperature surpasses 1204°C. Effect of cooling rate on ferrite level remains uninfluenced up to 1204°C, later the ferrite level increases beyond the amount present in the weld joint [49]. Below the temperature region of 7- solvus, ferrite reduction is consistent. It is impartial until a thermal cycle is not forced that raises the temperature above the 7-solvus. As the temperature increases above the 7-solvus, delta ferrite revives [51]. New delta ferrite will subdivide alloying elements in accord with the austenite and delta ferrite solubilities. This re-barriering will lower the assemblage of the "impurities" in the grain boundaries. Though, it may alter back to austenite during solidification [52].

2.5 Segregation of Alloying Elements

After initial solidification of a fully austenitic weld bead, "harmful" elements such as P, S, and Si segregates in the interdendritic regions. When the weld metal is reheated to a high temperature by a succeeding pass, grain boundary migration and grain growth eventuate. The grain boundaries moving through the material during grain growth have a tendency to "sweep up" and enhance the segregation of the deleterious species and to trap them in the grain boundaries [27]. Since diffusion is temperature and time dependent, diffusion magnifies by reheating and the occurrence of multiple thermal cycles exacerbates segregation.



Figure 7: Fine-Scale Dendritic, Faceted and Eutectic Structure Zone between Primary Dendrites [53]

The segregation of certain elements (P, S, and Si in particular) to grain boundaries is responsible for decreased ductility in Grade 304L ASSs. The segregation of nickel remains, reasonably weak, whether chromium and molybdenum suffer high secondary segregation due to the non-equilibrium distribution of alloy elements. Thus the formation of primary austenitic reduces segregation tendency of chromium and molybdenum and that of nickel increases during solidification [33]. Thus, it can be inferred that for primary ferritic solidification, the amount of segregation ratio for all other

constituents except for nickel is lower than the previous mode. The phenomenon of secondary dendrite arm coarsening also affect the progression of microsegregation. Secondary root factor is also solute transport/ redistribution and boundary movement that occurs at the solid/solid inter-phase interfaces during post solidification in the solid [57].

3. RESULTS AND DISCUSSIONS

HAZ cracks can widely be observed, principally, at the time of phase transformations in the solid state. Fissures occur in the Hazard HAZ region if the ferrite reduces below 1% in HAZ above 982°C whether the fully austenitic welds confine fissures due to base structure and the welding conditions employed. Hot cracking susceptibility can be attained by persisting FA / F solidification modes, whether the use of small weld deposits and Post-Weld Heat Treatment (PWHT) can lessen stress corrosion cracking by scattering the localized pressure by decreasing the quantity of the retained tensile strain possible to affect stress corrosion cracking. The quantity and distribution of delta ferrite, are powerfully controlled by the weld material composition, in compared to the cooling rate. The degree of degradation of the grain boundary ductility is dependent on the P, S, and Si contents coupled with the number of HAZ exposures. In the current review, it has been analysed that the extent of the "Hazard HAZ" region depends primarily on the weld metal chemistry as well as on Cr_{eq}/Ni_{eq} ratio combined with the Cr content, as well as on commission of Manganese and Molybdenum.

4. CONCLUSIONS

A thorough understanding of metallurgical developments in 304 steels is essential to employ them successfully. The assortment of suitable process parameters and joint preparation and fit-up reduces the risk of solidification cracking. A width/depth ratio of 0.5 is ordinarily best for resistance to solidification cracking. In the present work it was found that the stability of the austenite phase is primarily dependent on nickel content but enhances with a decrease in temperature. Literature review concludes that a minimum of ferrite number FN 4 and a maximum of ferrite number FN 8 in AISI 304 steel weld reduces the cracking susceptibility and advances the cracking resistance.

REFERENCES

1. Shankar V Peckner D and Bernstein I M, *Handbook of Stainless Steels*, McGraw-Hill, New York, (1977).
2. Saluja R.& Moeed K. M.,(2012). *The emphasis of phase transformations and alloying constituents on hot cracking susceptibility of type 304L and 316L stainless steel Welds*, *International journal of engineering science and technology*,4, 2206-16.
3. Olson D. L.,(1985). *Prediction of Austenitic Weld Metal Microstructure and Properties*, *Welding Journal*, 10, 281s–295s.
4. Vitek J. M., David S. A. & Hihman C. R., (2003). *Improved ferrite number prediction model that accounts for cooling rate effects—part 1: model development*, *Welding Journal*, 89, 10s–17s.
5. Lippold J. C., Baeslack W. A. & Varol I., (1992). *Heat affected zone liquation cracking in austenitic and duplex stainless steels*, *Welding Journal*, 1, 1-14.
6. Lippold J. C., (1994). *Solidification behavior & cracking susceptibility of pulsed-laser welds in austenitic stainless steels*, *Welding Journal*, 6, 129-39.
7. Anaele J. U., Onyemaobi O. O., Nwobodo C. S., & Ugwuegbu C. C., (2015). *Effect of electrode types on the solidification cracking susceptibility of austenitic stainless steel weld metal*, *International Journal of Metals*, 1-8.

8. Shankar V., Gill T. P. S., Mannan S. L. & Sundaresan S., *Solidification cracking in austenitic ss welds*, *Sadhana* 28 (2003) 359–82.
9. Tehovnik F., Petrovi D. S., Vode F., & Burja J., (2012). *Influence of molybdenum on the hot-tensile properties of austenitic stainless steels*, *Materials and technology*, 46, 649-55.
10. Asunción Valiente Bermejo M., (2012). *Reagent selection in austenitic stainless steel solidification modes characterization*, *Welding Journal*, 5, 133-40.
11. Castro D. B. V. et al., (2011). *Influence of annealing heat treatment and Cr, Mg, and Ti alloying on the mechanical properties of high-silicon cast iron*, *Journal of Materials Engineering and Performance*, 20, 1346–54.
12. Chandra K. et al., (2012). *Low temperature thermal aging of austenitic stainless steel welds: Kinetics and effects on mechanical properties*, *Materials science and engineering*, 534, 163-175.
13. Sasikala G. et al., (2013). *Characterisation of fatigue crack growth and fracture behaviour of SS 316L(N) base and weld materials*, *Advanced Materials Research*, 794, 449-59.
14. Garner F. A., (1997) *Irradiation creep and void swelling of austenitic stainless steels at low displacement rates in light water energy systems*. *Journal of Nuclear Materials*, 251, 252-61.
15. Bermejo M. A. V., (2012). *Predictive and measurement methods for delta ferrite determination in stainless steels*, *Welding Journal*, 91, 113-21.
16. Jones H., (1984). *Microstructure of rapidly solidified materials*, *Materials Science and Engineering*, 65, 145-56.
17. Cross C. E., Grong O., Liu S., & Capes J. F., (1986). *Metallography and Welding Process Control*, In: Vander Voort G. F. (eds) *Applied Metallography*, Springer, Boston, MA.
18. Nakano J., Miwa Y., Kohya T. & Tsukada T., (2004). *Effects of silicon, carbon and molybdenum additions on IASCC of neutron irradiated austenitic stainless steels*, *Journal of Nuclear Materials*, 329-333, 643 – 647.
19. Coniglio N., Cross C. E., Schempp P. & Mousavi M. (2008). *Defining a critical weld dilution to avoid solidification cracking in Aluminum*, *Welding Journal*, 9, 237-47.
20. Zhuang C., Li Z., & Lin S., (2015). *Counter-intuitive experimental evidence on the initiation of radical crack in ceramic thin films at the atomic scale*, *AIP Advances*, 5, 107231-37.
21. Kujanpaa V. P., David S. A. & White C. L., (1986). *Formation of Hot Cracks in Austenitic Stainless Steel Welds—Solidification Cracking*, *Welding Journal*, 8, 203-212.
22. Sourmail T., (2001). *Precipitation in austenitic stainless steel*, *Material science and technology*, 17, 1- 14.
23. Lundin C. D., Chou C. P. D. & Sullivan D. J., (1980). *Hot cracking resistance of austenitic stainless steel weld metals*, *Welding Journal*, 59, 226–32.
24. Gooch T. G. & Honeycombe J., (1980), *Welding variables and microfissuring in austenitic stainless steel weld metal*, *Welding Journal*, 8, 233-241.
25. Gowrisankar I., (1987). *Effect of the number of passes on the structure and properties of submerged arc welds of AISI Type 316L stainless steel*, *Welding Journal*, 5, 147-54.
26. Fredriksson H., (1982). *Solidification of iron base alloy*, *Metal science*, 16, 575-586.
27. Hull F. C., (1973). *Effects of composition on embrittlement of austenitic stainless steels*, *Welding Journal*, 3, 104–13.

28. Lundin C. D.,(1976). *The Nature and Morphology of Fissures in Austenitic Stainless Steel Weld Metals*, *Welding Journal*, 11, 356-67.
29. Lundin C. D.,(1985). *Fissuring in the hazard HAZ region of austenitic stainless steel welds*, *Welding Journal*, 4, 113-18.
30. Noecker II F. F.& Dupont J. N., (2009). *Metallurgical investigation into ductility dip cracking in Ni-based alloys: Part II*, *Welding Journal*, 88, 62-77.
31. Yoo J., Kim B., Jeong Y., Park Y.& Lee C.,(2015). *Influence of Cr on Weld Solidification Cracking in Fe-15Mn-0.5C- 3.5Al-xCr Alloys*, *ISIJ International*,55, 257–263.
32. Ohmori Y.& Kunitake T.,(1983). *Effects of austenite grain size and grain boundary segregation of impurity atoms on high temperature ductility*, *Metal Science*, 17, 325-332.
33. Mohammed G. R., Ishak M., Aqida S. F.& Abdulhadi Hassan A.,(2017). *Effects of Heat Input on Microstructure, Corrosion and Mechanical Characteristics of Welded Austenitic and Duplex Stainless Steels: A Review*, *Metals*, 7, 39-56.
34. Tavares S. S. M. et al.,(2017). *Influence of Microstructure on the Corrosion Resistance of AISI 317L (UNS S31703)*, *Material Research*, 1-7.
35. Ramkumar K. D.,(2014) *Hot corrosion behavior of monel 400 and AISI 304 dissimilar weldments exposed in the molten salt environment containing Na₂SO₄ + 60% V₂O₅ at 600 °C*, *International Journal of Plasticity, Materials Research*, 17,1273-84.
36. Corradini M. L., Kim B. J.,& Oh M. D.,(1988). *Vapor explosions in light water reactors: A review of theory and modeling*, *Progress in Nuclear Energy*, 22, 55.
37. Kujanpaa V. P.,(1987). *Weld discontinuities in austenitic stainless steel sheets*, *Welding Journal*, 06, 155-61.
38. Du Toit M., Rooyen G. T. V.& Smith D.,(2007). *Heat-affected zone sensitization and stress corrosion cracking in 12% chromium type 1.4003 ferritic stainless steel*, *Corrosion*, 63,395-404.
39. Li L.,& Messler R. W.,(2002). *Segregation of Phosphorus and Sulfur in Heat-Affected Zone Hot Cracking of Type 308 Stainless Steel*, *Welding Journal*, 5,78-84.
40. Osoba, L., Ekpe, I., & Elemuren, R. *Analysis Of Dissimilar Welding Of Austenitic Stainless Steel To Low Carbon Steel By Tig Welding Process*.
41. Ogawa T.& Tsunetomi E., (1982). *Hot cracking Susceptibility of austenitic stainless Steels*, *Welding Journal*, 3, 82-93.
42. Bhadeshia H. K. D. H.,(2016). *Prevention of Hydrogen Embrittlement in Steels*, *ISIJ International*, 56 24-36.
43. Saluja R.& Moeed K. M.,(2014) *Emphasis of embrittlement characteristics in 304L and 316L austenitic stainless steel*, *IOSR Journal of Mechanical and Civil Engineering*, 11, 04-10.
44. Povich M. J.& Rao P.,(1978). *Low Temperature Sensitization of Welded Type 304 Stainless Steel*, *Corrosion*, 34, 269-275.
45. Terada M., Saiki M., Costa I.,& Padilha A. F.,(2006). *Microstructure and intergranular corrosion of the austenitic stainless steel 1.4970*, *Journal of Nuclear Materials*, 358, 40–46.
46. Kobayashi D. Y.& Wolyneec S.,(1999). *Evaluation of the Low Corrosion Resistant Phase Formed During the Sigma Phase Precipitation in Duplex Stainless Steels*, *Material Research*, 2, 239-247.
47. Soriano-Vargas, Davila E. O. A., Hirata V. M. L.& Rosales H. J. D., Velazquez J. L. G.,(2009). *Spinodal decomposition in an Fe-32 at%Cr alloy during isothermal aging*, *Materials transactions*, 50, 1753- 57.

48. Adamson M. G., Aitken E. A. & Vaidhyanathan S.,(1982). Synergistic tellurium–caesium embrittlement of type 316 stainless steel, *Nature*, 295, 49–51.
49. Kang M., Zhang M. X., Liu F. & Zhu M.,(2009). Kinetics and Morphology of Isothermal Transformations at Intermediate Temperature in 15CrMnMoV Steel, *Materials Transactions*, 50, 123-29.
50. Neustroev V. S. & Garner F. A.,(2008). Very high swelling and embrittlement observed in a Fe-18Cr-10Ni-Ti hexagonal fuel wrapper irradiated in the bor-60 fast reactor, *Journal Of nuclear materials*, 378, 327-32.
51. Romanczuk E., & Oksiuta Z.,(2017). Comparison of corrosion resistance in physiological saline solution of two austenitic stainless steels – 316LV and REX734, *Acta mechanica et automatic*, 11, 91-95.
52. Vodopivec F.,(2004.) Strain ageing of structural steels, *Metalurgija*,43, 143-48.
53. Rashid M W A, Gakim M, Rosli Z M & Azam A, Formation of Cr23C6 during the Sensitization of AISI 304 Stainless Steel and its effect to pitting corrosion, *Int. J. Electrochem. Sci.* 7 (2012) 9465– 77.
54. Vitek J. M. & David S. A.,(1986). The Sigma Phase Transformation in Austenitic Stainless steel, *Welding Journal* 4 106-115.
55. Savage W. F., Nippes E. F., Mushala M. C.,(1978). Liquid metal embrittlement of the heat-affected zone by copper contamination, *Welding Journal*, 8, 237-45.
56. Rao A. C. U. et al., (2016). Stress corrosion cracking behaviour of 7XXX aluminum alloys: A literature review, *Transactions of Nonferrous Metals Society of China*, 26, 1447-71.
57. Pan C et al., (2003). Hydrogen embrittlement induced by atomic hydrogen and hydrogen-induced martensites in type 304L stainless steel, *Mat. Sci. and Engineering*, 351, 293-98.
58. Gavriljuk V. G., Shivanyuk V. N., & Foct J., (2003). Diagnostic experimental results on the hydrogen embrittlement of austenitic steels, *Acta Materialia*, 51, 1293-1305.
59. Perng T. P., Johnson M. & Altstetter C. J., (1989). Influence of plastic deformation on hydrogen diffusion and permeation in stainless steels, *Acta Metallurgica*, 37, 3393-97.
60. Shivanyuk V. N. et al.,(2001). Effect of hydrogen on atomic bonds in austenitic stainless steel, *Scripta Materialia*, 44, 2765-73.
61. Bak S. H., Abro M. A., & Lee D. B., (2016). Effect of hydrogen and strain-induced martensite on mechanical properties of AISI 304 stainless steel. *Metals*, 6, 169-77.
62. Turnbull A.,(1993). Modelling of environment assisted cracking, *Corrosion Science*, 34, 921-60.
63. Thompson A. W., (1973). Hydrogen embrittlement of stainless steels by lithium hydride, *Metallurgical Transactions*, 4, 2819–2825.
64. Zhang L. et al., (2012). Internal reversible hydrogen embrittlement of austenitic stainless steels based on type 316 at low temperatures, *ISIJ International*,52, 240–46.
65. Kumar S. & Curtin W. A., (2007). Crack interaction with microstructure. *Materials today*, 10, 34-44.
66. Ferrandini P. et al., (2006). Solute segregation and microstructure of directionally solidified, austenitic stainless steel, *Materials Science and Engineering*, A435-436, 139-144.

